# Determination of Moisture Diffusivity for Unsaturated Fractured Rock Surfaces

Robert C. Trautz and Steve Flexser

Lawrence Berkeley National Laboratory, 1 Cyclotron Rd., 90R1116, Berkeley, CA, USA 94720
(510) 486-7954, rctrautz@lbl.gov

## Introduction

Trautz and Wang (2002) described a series of field experiments performed in an underground test facility constructed in an unsaturated, fractured volcanic tuff located at Yucca Mountain, Nevada. The primary purpose of the testing program was to determine whether water percolating down from the land surface through the unsaturated zone would be diverted around an underground tunnel because of the existence of a capillary barrier at the tunnel ceiling. Trautz and Wang (2002) showed that by releasing water in boreholes located above a 3.25 meter (m) high by 4 m wide drift, a capillary barrier is revealed, leading to lateral flow of water around the opening.

The seepage tests described by Trautz and Wang (2002) provide a unique opportunity to observe the arrival and movement of water across a suspended, unsaturated fractured rock surface. The spread of water from its initial point of arrival at the tunnel surface across the ceiling will be used in this paper to estimate the moisture diffusivity, $D(\theta)$, along the ceiling surface and adjacent rock.

## Test Description and Observations

Water was released at a constant rate over a 2-day period into a 0.3 m section of borehole UL, installed 0.7 m above the tunnel (Figure 1). Fractures intersecting the test interval conducted water from the borehole to the tunnel ceiling, where it initially appeared as isolated wet spots (Points 1 and 2 on Figure 2). The capillary barrier prevented water from immediately dripping into the opening, causing the water to spread laterally across the ceiling. Its advance was recorded using time-lapse video, allowing the position of the wetting front to be mapped from the resulting images. Figure 2 shows the position of the wetting front 1, 3, 8, 18, 28, and 48 hours after arriving at the ceiling. Despite the presence of numerous visible fractures and irregularities in the ceiling surface, the wetting front spread in a surprisingly homogenous, radial symmetric pattern. The equivalent radial distance ($r_f$) that the wetting front has traveled from the point of first arrival (assuming a radial flow field) is calculated as $r_f = (A/\pi)^{1/2}$, where A is the area of the wetted rock contained within the boundaries of the wetting front (Figure 3).

Eventually, the rock surface became saturated near the location of the first arrival and water dripped or seeped into the tunnel. Seepage typically takes place from topographic low points on the ceiling surface in close proximity to the first-arrival location. The position of the wetting front at the time that dripping started (8 hours after the first arrival) is shown as a dashed line and individual drip locations (48 hours after first arrival at the end of the test) are shown as x's in Figure 2. The wetting front continued to spread as long as water was supplied to the ceiling from the overlying borehole. The measured release rate into the test borehole, the seepage rate into the opening, and the supply rate are plotted in Figure 3. Note that the supply rate is defined as the difference between the release and seepage rates and, therefore, represents the amount of water feeding or supplying the advancing wetting front (assuming negligible evaporation).

## Conceptual Flow Model

The observations described above can be conceptualized as two unsaturated flow processes that are commonly described in the soil physics literature. The first process, *infiltration*, occurs

when water is released into the borehole located above the opening and infiltrates through vertical fractures to the tunnel ceiling. Trautz and Wang (2002) determined that the capillary strength of the fractures associated with the test was very weak, and they concluded that infiltration through the fracture system was predominately a gravity-driven (as opposed to a capillary-driven) process.

The second process, spreading, is analogous to horizontal absorption described by Philip (1969) for soils. It begins once the wetting front reaches the relatively flat, horizontal ceiling and begins to move or spread laterally. During the earliest stage of spreading, the rate that water is supplied to the ceiling may be less than that being released to the overlying borehole because of a time lag for the infiltration flux to fully reach the ceiling. At later stages, the supply rate may equal the release rate, creating a constant flux inner boundary condition as the wetting front advances. This is shown conceptually as a zone of "increasing flux" ($r < r_o$) on Figure 4.

As time progresses, the rock surface becomes saturated, and dripping begins when the supply rate at the tunnel ceiling exceeds the rate that water can be transmitted laterally through the matrix, fractures, and along surface films that develop at the tunnel-wall rock interface. It is at this point that the boundary condition changes from one of increasing or near-constant flux to one of constant water content, $\theta$ (Figure 3 and 4). The wetting front advances under constant $\theta$ conditions from this point forward. However, it should be noted that the supply rate may continue to change for a period of time after dripping begins (Figure 3) as the initially strong capillary forces diminish with time. The time required to reach constant-$\theta$ conditions is often referred to in the literature as the "time to ponding" ($t_p$), and the radial distance ($r_o$) at which this transition from constant flux to constant-$\theta$ conditions first occurs is defined herein for our radial model as the equivalent radial distance that the wetting front has traveled when dripping begins (Figure 4). This occurs at $r_f = r_o = 212$ mm (Figure 3) and corresponds to the actual wetting-front position shown by the dashed line on Figure 2. It is important to realize that $r_o$ represents the approximate radius of the constant-$\theta$ supply surface or source.

## Data Analysis

Philip (1969) and many others have published a number of solutions to the equation governing unsaturated water movement through nonswelling soils for a homogeneous, semi-infinite medium with a constant-$\theta$ condition at the fixed boundary. Exact and/or approximate solutions have been derived for infiltration and absorption from 1-D surfaces, 2-D cylinders, and 3-D spheres (Philip 1969). Philip (1968) derived the following dimensionless solution for a step increase in $\theta$ at the cylindrical supply boundary ($r_o$) of a horizontal 2-D radial flow domain:

$$T = \frac{2}{\pi}\left[(1+2I)\log(1+2I) - 2I\right] \tag{1}$$

where

$$T = \frac{D\,t}{r_o^2} \qquad \text{and} \qquad I = \frac{r_f - r_o}{r_o} \tag{2}$$

and D is the moisture diffusivity [$m^2$/seconds (s)], t is time [s], and $r_o$ and $r_f$ are the radial distance [m] to the water supply and wetting front boundaries, respectively, defined earlier. The solution above uses the same plug-type flow condition originally developed by Green and Ampt (1911) for vertical infiltration. It assumes that the wetting front advances as a "square wave" with a "sharp" wetting front (i.e., infinitely steep water potential gradient). The water content behind the wetting front is everywhere the same and equal to the water content imposed at the water supply boundary, $\theta_o$, at t = 0. Therefore, D takes on a constant value $D(\theta_o)$ and drops instantaneously at the wetting front to $D(\theta_i)$ where $\theta_i$ is the ambient water content of the medium at initial condition

$t \leq 0$. Green and Ampt-type solutions have been shown to predict infiltration and absorption reasonably well for early times for very dry and/or coarse media. Distinct, sharp (i.e., not diffused) wetting fronts were observed during the seepage tests, providing qualitative support for the use of (1) to analyze the $r_f$ –derived data in Figure 3.

## Conclusion

Equation (1) was used to derive the type-curve shown on Figure 5 for an arbitrary set of I and T. The radius of the water supply $r_o$ and equivalent radial front position $r_f$ shown on Figure 3, and the corresponding elapsed time from the start of ponding (t) for each front position, were substituted, along with an initial guess for D into (2) to produce I and estimates of $T = T_{est}$. The resulting value of I was then substituted into (1) to produce predicted values of $T = T_{pred}$. The optimum value of D was determined by repeating the process, iteratively using successive values for D that minimized the sum of residuals ($T_{pred} - T_{est}$) squared as follows:

$$\text{Minimize} \quad \sum_{n=1}^{\#\ of\ Data} \left(T_{pred,n} - T_{est,n}\right)^2 \tag{3}$$

The final fit of the data, compared to the analytical solution in Figure 5, produces a value of moisture diffusivity D equal to 3.2E-7 $m^2/s$. This value agrees with measured 1-D surface film diffusivities reported by Tokunaga et al. (2000) equal to 3.2E-7 and 1.7E-7 $m^2/s$ for a glass cast of a granite fracture and roughened glass surface, respectively. This leads us to believe that the primary mechanism for wetting-front movement across the ceiling is by surface film flow. This is substantiated by the fact that preferential flow along visible fractures is not evident in the wetting patterns of Figure 2, suggesting that visible fractures do not control the wetting process (other than to serve as the water source from above). Vertical absorption from the advancing wetting front into the overlying rock matrix could also influence the process by contributing to the "sharpness" of the observed wetting front. However, behind the front, this process is expected to be relatively minor. This is because the rock matrix diffusivity drops rapidly at the wetting front, where the water-potential gradient is very steep, to a very low value behind the front, where the gradient decreases quickly because of the very low conductivity of the matrix (4.0E-11 m/s, Flint 1998). The low conductivity of the matrix causes saturated conditions to develop quickly in the matrix at the ceiling surface-rock matrix interface. The corresponding rapid reduction in the water-potential gradient and rate of absorption into the matrix allows surface films to persist at water potentials perhaps as large as -100 kPa in our case (Figure 4 in Tokunaga and Wan, 2001).

## References


Flint , L.E., Characterization of hydrogeologic units using matrix properties, Yucca Mountain, Nevada, *U.S. Geol. Sur. Water Resour. Invest. Rep., 97-4243*, 64 pp., 1998.

Green, W.H. and G.A. Ampt, Studies of soil physics: Part I – The flow of air and water through soils, *J. Agricultural. Sci.*, Vol. IV, 1-24, 1911.

Philip, J.R., Theory of Infiltration, *Adv. Hydrosci., 5*, 215-295, 1969.

Philip, J.R., Absorption and infiltration in two- and three-dimensional systems, in *Water in the Unsaturated Zone*, *Proceedings of the Wageningen Symposium 1966, Vol. 1*, published by IASH/UNESCO, Paris, France, 503-516, 1968.

Trautz, R.C. and J.S.Y. Wang, Seepage into an underground opening constructed in unsaturated fractured rock under evaporative conditions, *Water Resourc. Res.*, *38*(10), 6-1 – 6-14, 2002.

Tokunaga, T.K., J. Wan, and S.R. Sutton, Transient film flow on rough fracture surfaces, *Water Resourc. Res.*, *36*(7), 1737 – 1746, 2000.

Tokunaga, T.K. and J. Wan, Approximate boundaries between different flow regimes in fractured rocks, *Water Resourc. Res.*, *37*(8), 2103 – 2111, 2001.

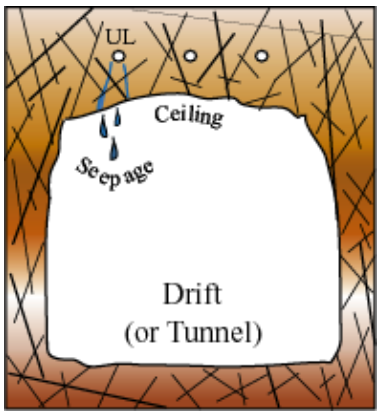


**Figure 1. Test configuration.**

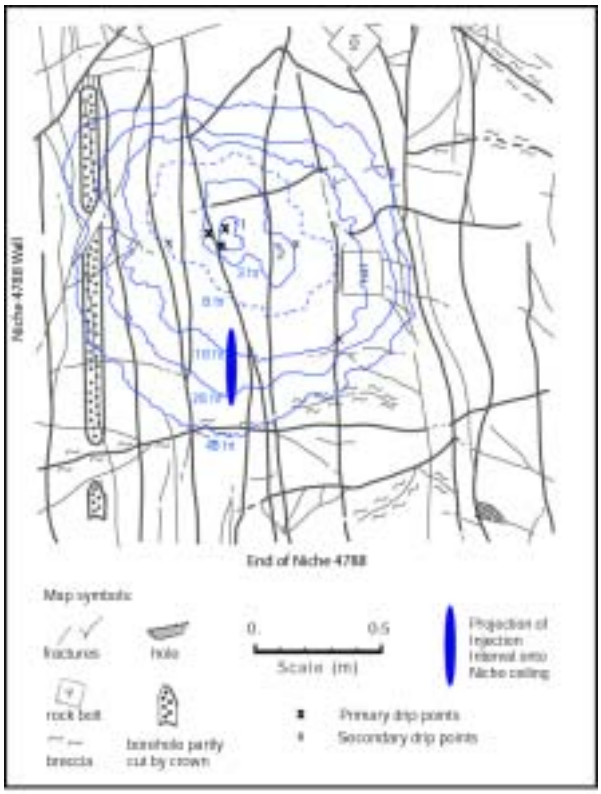


**Figure 2. Spread of the wetting front across the tunnel ceiling. Front positions are shown 1,3 ,8, 18, 28 and 48 hours after the first arrival (contour labeled 1 and 2).**

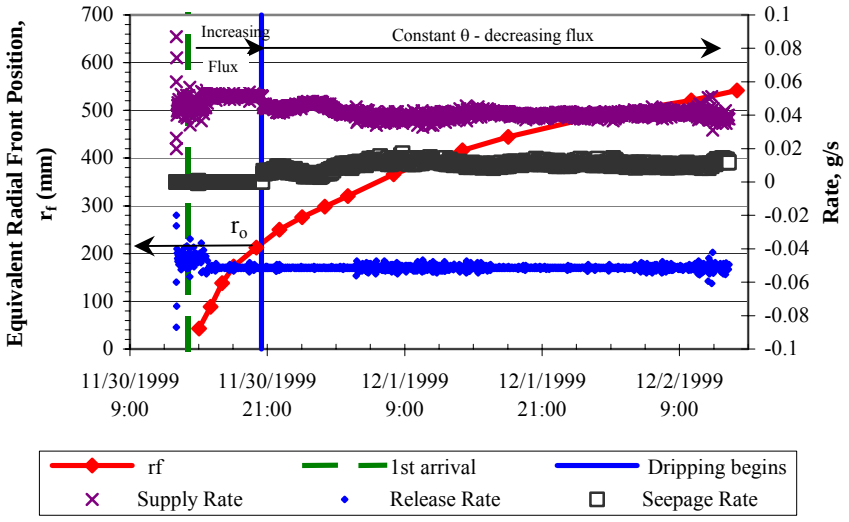


**Figure 3. Wetting front radial position and release, seepage and supply rates for test.**

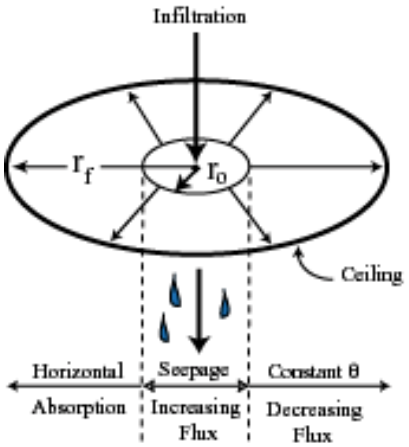


**Figure 4. Conceptual flow model showing 2-D radial absorption along horizontal surface of tunnel ceiling.**

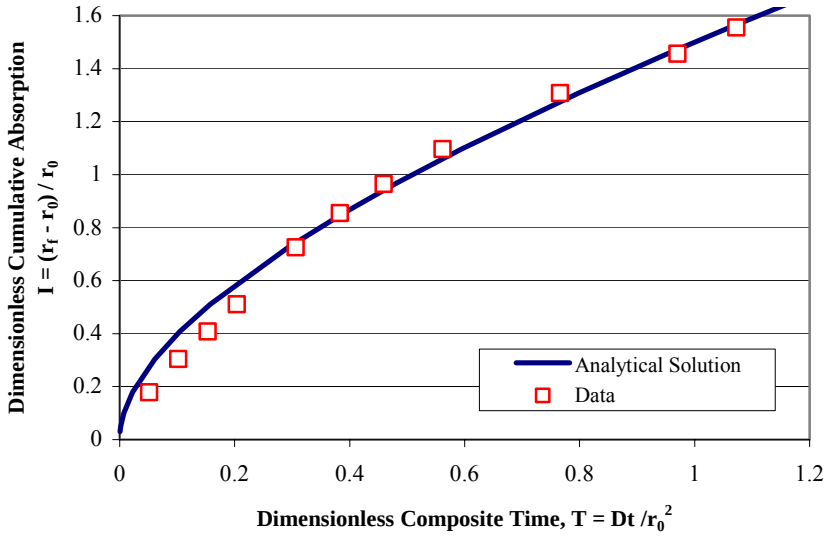


**Figure 5. Best fit of data to analytical solution (Philip 1986) using moisture diffusivity D(θ) equal to 3.2E-07 $m^2/s$.**